A Novel Modelling Approach to Energy Transport in a Respiratory System.

Perumal Nithiarasu* and Igor Sazonov
Biomedical Engineering and Rheology Group
Zienkiewicz Centre for Computational Engineering
College of Engineering, Swansea University, UK

Abstract

In this paper, energy transport in a respiratory tract is modelled using the finite element method for the first time. The upper and lower respiratory tracts are approximated as a one-dimensional domain with varying cross sectional and surface areas and the radial heat conduction in the tissue is approximated using the one dimensional cylindrical coordinate system. The governing equations are solved using one-dimensional linear finite elements with convective and evaporative boundary conditions on the wall. The results obtained for the exhalation temperature of the respiratory system have been compared with the available animal experiments. The study of a full breathing cycle indicates that evaporation is the main mode of heat transfer and convection plays almost negligible role in the energy transport. This is inline with the results obtained from animal experiments.

keywords: respiratory system, heat transfer, convection, evaporation, finite element method, stabilised method.

1 INTRODUCTION

The surface area of human respiratory tract varies between 30 and 100 m^2. This provides a surface to volume ratio of between 5000 and 17000 m^2/m^3. Such large values clearly make the human respiratory tract extremely efficient in heat and mass transport. Since mass exchange is the primary function of lungs, a large number of studies have focused on this subject. Although the energy transport is the secondary function of a respiratory tract, this is a very important function to regulate thermal balance of a body. In some animals this is one of the main method of maintaining thermal equilibrium. One of the prominent features of lungs is that approximately 700 million interconnected alveolar sacs exchange heat and gas with blood. A typical alveolus is about 200μm in size.The blood capillaries surrounding these alveolar sacs efficiently transfer carbon dioxide and heat to the air via the respiratory system. Since the temperature at the interface between blood and alveoli is approximately equal to the body temperature, the heat transfer coefficient between the alveolus and air may be calculated to be between 0.2 and 5 $W/m^{2o}C$. This clearly shows that the heat transfer coefficient is lower than that of natural convection range, yet the lung is very efficient in transferring energy. Due to the highly efficient nature of heat exchange in the respiratory tracts, potential for developing compact heat exchangers by studying them in depth is high. Since engineers consider a heat exchanger with a surface to volume ratio of more than $700m^2/m^3$ as a compact heat exchanger, the respiratory tract truly is such a heat exchanger. Some recent studies indicate that exhalation temperature of a respiratory tract may provide some indication of lung pathology. Thus, understanding the energy transport

*Correspondence to: P. Nithiarasu, Website: http://www.swansea.ac.uk/staff/academic/engineering/nithiarasuperumal/ email: P.Nithiarasu@swansea.ac.uk

within a respiratory tract may be of great interest to heat exchanger researchers, biologists, ear, nose and throat (ENT) and chest clinicians and biomedical engineers.

Many researches have attempted to measure the exhalation temperature of both humans and animals[1, 2]. It appears that the exhalation temperature may be used as a biomarker for detecting disorders of a respiratory system. For example, in asthma patients, inflammation increases the perfusion in the airway walls and thus more heat exchange is expected between the blood and air, resulting in a higher exhalation temperature than normal. This hypothesis has been tested by many researchers by measuring the exhalation temperature and correlating it against nitric oxide (NO). The correlation is very encouraging and it appears that the exhalation temperature of asthma patients is higher than that of normal subjects [3, 4, 5, 6, 7, 8]. These works have demonstrated that the temperature may be used as a biomarker to determine the severity of disorders such as asthma or chronic obstructive pulmonary disease (COPD) [9]. Such studies have been complemented by development of temperature measurement techniques and devices [10]. Both the potential of using lung biomimetics to develop compact heat exchangers and using exhalation temperature as a biomarker have motivated the present modelling work. Developing a robust computational model for airway may provide further insight into the heat transfer mechanism and allow us to manipulate important parameters. For example, by changing the respiratory tract wall heat transfer coefficient one can easily account for increase or decrease in heat transfer between blood and air.

A computational model of respiratory tract may be developed using three different approaches. The first and most simple approach is empirical or lumped model approach in which correlations or zero dimensional models are used to analyse the heat exchange[2, 11, 12, 13]. Although the lumped model is useful to study experimental measurements and simple scenarios, it is not a robust model for predicting temperature distribution in space and time. A more robust model may be constructed using a one-dimensional tree with fluid-structure interaction models[14, 15] similar to blood flow analysis[16]–[28]. Such a model is very useful when local flow distribution is of interest. The one-dimensional fluid-structure interaction has been extensively and successfully used in systemic blood flow calculation to compute temperature[29, 30]. For much more comprehensive and detailed study, a full three dimensional model may be employed. A fully three dimensional model of the entire respiratory tract is extremely complex to build and thus many authors have only focused on the upper part of the respiratory tract [31, 32, 33, 34, 35] although comprehensive lower airway models have been recently investigates[36, 37]. While one-dimensional fluid-structure interaction model can give a better result than the lumped models and the three-dimensional models can give every details of the flow, both these approaches can be extremely difficult to implement to capture the details. Since the temperature distribution in the respiratory tract is governed by a convection-diffusion equation, an approximate way of including the velocity distribution with time and space may be sufficient to obtain an accurate temperature distribution. Thus, a one-dimensional spatial model for temperature with varying cross section is proposed along with a finite element solution method to solve the mathematical model.

The heat transfer mechanisms in respiratory tract include convective and latent heat losses (evaporation)[2]. The convective part is a result of the temperature difference between the wall and air. An appropriate value of heat transfer coefficient for forced convective heat transfer between the wall and air needs to be included. The evaporative heat transfer is the result of evaporation/condensation of airway surface water. The experimental work carried out on animals indicate that evaporative part is the dominant mode of heat transfer[2]. In addition to the model, including both convective and evaporative boundary conditions, a velocity wave form needs to be prescribed along with an inlet temperature boundary condition at the inlet (note that the inlet is also the exit). These boundary conditions should be incorporated into a convective-diffusive transport system to determine the temperature distribution in the air. Since the respiratory tract wall temperature will be influenced by the inhaling air temperature, assuming a fixed wall temperature along the tract will be incorrect. Thus, a conjugate heat transfer mechanism should be included by incorporating the heat conduction in the surrounding soft tissue. To accurately model the heat conduction in the surrounding, the tissue should be modelled using bioheat equations. Since the perfusion rates, metabolism and other details in and around airway are difficult to determine, it may be possible to assume a small wall thickness with pure heat conduction. The outer surface of the wall may be assumed to be at a temperature equal to the body temperature. Due to the large surface area of the alveolar sacs, the temperature at the gas exchange

interface may be assumed to be equal to the body temperature. With the mentioned assumptions, a robust model may be constructed to study the heat transport in respiratory tracts.

The paper is organised into the following sections. In the section that follows the introduction, we develop the mathematical model in detail. In Section 3, the convection-diffusion equation is solved using a stabilized finite element method. The results are discussed in detail in Section 4 and Section 5 derives some important conclusions.

2 MATHEMATICAL MODEL

The two main mechanisms of heat transfer in a respiratory tract are convection and latent heat of evaporation from the wall. The convective heat transferred from or to the respiratory tract walls may be written as [38]

$$Q_c = hPL(T_w - T_a) \tag{1}$$

where h is the heat transfer coefficient, P is the perimeter, L is the length of the passage along which heat is transferred, T_w is the wall temperature and T_a is the local air temperature. In a lumped fashion the heat transfer due to convection may be written as

$$Q_c = \dot{m}c_p(T_b - T_{ai}) \tag{2}$$

where $\dot{m}$ is the mass flow rate, T_b is the body temperature and T_{ai} is the inlet air temperature (ambient temperature). Heat transfer as a result of latent heat of vaporisation may be written as [39]

$$Q_L = \frac{\lambda\dot{m}}{\rho_a}(\phi_e - \phi_i) \tag{3}$$

where λ is the latent heat of water evaporation, ρ_a is the density of air and ϕ_e and ϕ_i are the absolute humidities of expired and inspired air respectively. The absolute humidities may be defined as

$$\phi_e = \frac{10^3 M_w e^*}{RT_b} \tag{4}$$

and

$$\phi_i = \frac{10^3 M_w e}{RT_b} \tag{5}$$

where M_w is the mol mass of water (18.016 g/mol), R is the molar gas constant (8.3143 J/Mol K), e^* (kPa) is the saturation vapour pressure of the air at T_b and e (kPa) is the partial vapour pressure of air at T_a[40]. The vapour pressures may be calculated as [41, 2]

$$e(T) = 0.61075 \times 10^{\left\{\frac{7.5T}{T+237.5}\right\}} \tag{6}$$

The total heat transferred in a respiratory tract is therefore $Q = Q_c + Q_L$[41].

Although the above lumped model is useful to study different scenarios, it is not a robust model for predicting temperature distribution in space and time. A time dependent model in three dimensions will be the most comprehensive model for a respiratory system. However, the structural complexities of lungs can be extremely difficult to deal with using three dimensional spatial models. The one-dimensional models on the other hand are simple, fast and they can provide a good overall approximation of the reality. The one-dimensional energy equation governing temperature distribution (in degree Celsius) in a human respiratory tract may be written for air as[38]

$$\rho_a c_{pa} A_c \left(\frac{\partial T}{\partial t} + u\frac{\partial T}{\partial x}\right) - \frac{\partial}{\partial x}\left(k_a A_c \frac{\partial T}{\partial x}\right) + hP_a(T - T_w) + \frac{\lambda\dot{m}}{l\rho_a}(\phi_b - \phi_a) = 0 \tag{7}$$

where c_{pa} is the specific heat of air at constant pressure, A_c is the cross sectional area, u is the velocity of air, k_a is the thermal conductivity of air, P_a is the perimeter, T_w is the wall temperature, l is the length of the section in which energy is balanced, ϕ_b is the local body humidity and ϕ_a is the local air humidity . Since the respiratory tract wall temperature is not constant, a model to determine the wall temperature is essential. The simplest form of heat conduction model is a one-dimensional model in the radial direction originating from the respiratory tract wall. Such a model for heat conduction through the wall to determine the tissue temperature may be written as

$$\rho_t c_{pt} A_r \frac{\partial T}{\partial t} - \frac{\partial}{\partial x}\left(k_t A_r \frac{\partial T}{\partial x}\right) + \left[hA_r(T - T_a) + \frac{\lambda \dot{m}}{\rho_t}(\phi_A - \phi_e)\right]_{interface} = 0 \tag{8}$$

where subscripts t and r indicates tissue and radial direction respectively. In the above equation, A_r is the area in the radial direction and this area is calculated using the radii along the respiratory tract and it varies depending the radial distance from the airway surface into the tissue. It should also be noted that the last two terms in Equation 8 are only used as the boundary conditions at the interface between air and tissue.

3 STABILIZED FINITE ELEMENT METHOD

Equation 7 along with appropriate initial and boundary conditions is solved in the present work using an explicit Taylor Galerkin (TG) method and the heat conduction equation 8 is solved using standard explicit Galerkin method[38, 42]. The TG method in its semi-discrete from may be written as

$$\begin{aligned} \rho_a c_{pa} A_c \left(\frac{T^{n+1} - T^n}{\Delta t}\right) &= \\ &- \rho_a c_{pa} A_c u \left(\frac{\partial T}{\partial x}\right)^n + \frac{\partial}{\partial x}\left(k_a A_c \frac{\partial T}{\partial x}\right)^n \\ &+ \frac{u^2 \Delta t}{2}\left(\frac{\partial^2 T}{\partial x^2}\right)^n - hP_a(T - T_w)^n - \frac{\lambda \dot{m}}{\rho_a l} P(\phi_b - \phi_a)^n \end{aligned} \tag{9}$$

where superscripts n and $n+1$ indicates the current and next time levels between a time step Δt. The TG effect due to convection term is retained and all other higher order terms are neglected. Assuming that the flow is incompressible and the velocity is one-dimensional and vary only as a function of cross sectional area, the temperature may be spatially discretized using linear finite elements as $\mathbf{T}^{(e)} = N_1 T_1 + N_2 T_2$ in which superscript (e) indicates a linear element, N_1 N_2 are the linear shape functions and T_1 and T_2 are the nodal temperature values. The standard Galerkin weighting of Equation 9 along with the linear temperature discretization results in the following final matrix form of the convection-diffusion equation.

$$\mathbf{M}\left(\frac{\Delta \mathbf{T}}{\Delta t}\right) = -\mathbf{C}\mathbf{T}^n - \mathbf{K}\mathbf{T}^n - \mathbf{K_s}\mathbf{T}^n - \mathbf{M_c}\mathbf{T}^n + \mathbf{F}^n \tag{10}$$

where $\mathbf{M}$ is the mass matrix, $\mathbf{C}$ is the convection matrix, $\mathbf{K}$ is the diffusion matrix, $\mathbf{K_s}$ is the starbilization matrix, $\mathbf{M_c}$ is the modified mass matrix for the interface convection term and $\mathbf{F}$ contains all the boundary conditions and evaporation term. Further details on the matrices can be found in standard finite element text books on fluid dynamics [38, 42]. In a similar fashion, Equation 8 is solved using standard Galerkin finite element method and linear elements.

3.1 Boundary conditions, solution sequence and convergence

As seen in Equations 7 and 8, the interface is linked through convective and evaporative heat transfer boundary conditions. Figure 1 (b) shows the approximate model of the respiratory tract along with the

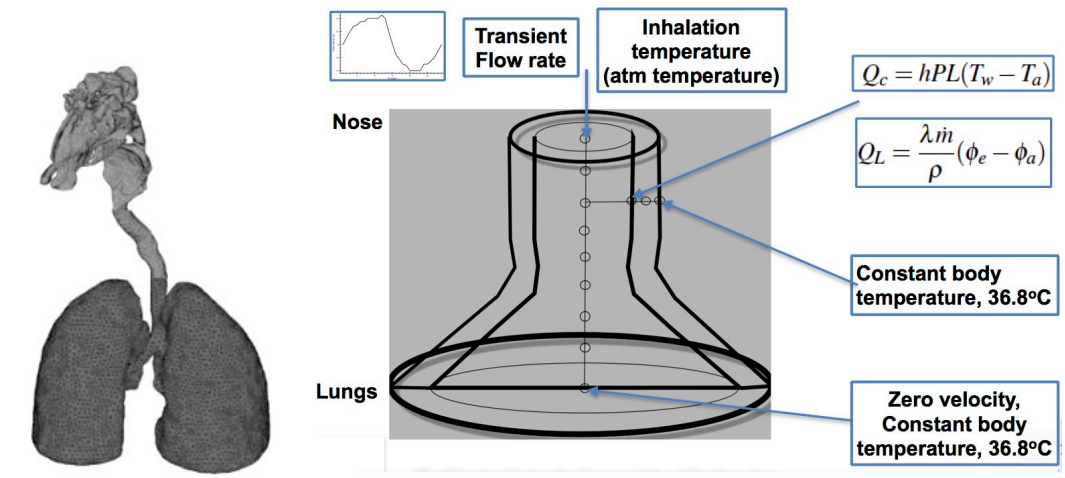

(a) Typical respiratory tract

(b) Approximate geometry and boundary conditions

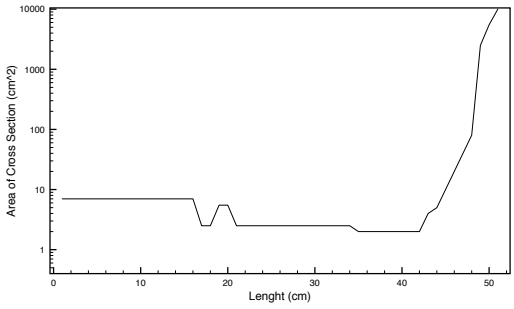

(c) Variation of cross sectional area

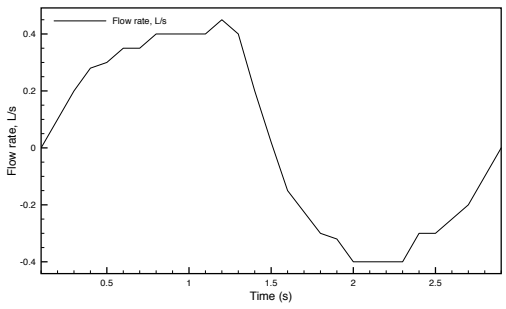

(d) Flow rate variation with time

Figure 1: Airway geometry details, approximation and flow rate.

boundary conditions. The convective and evaporative conditions for the temperature transport in the air (Equation 7 is applied all along the wall surface, i.e., to every finite element along the respiratory tract). However, the convective and evaporative condition for the heat conduction in the tissue, along the radial direction is only applied at the interface between the air and tissue. Also, every air node will have a solid domain in the radial direction.

As seen in Figure 1(b), for the air side, a breathing flow rate cycle is imposed at the inlet/exit, and at the interface between the air and wall, a convective heat transfer surface condition is imposed in addition to the evaporative condition. At the lung end of the tract, the temperature is assumed to be that of the body temperature at 36.8^o C. As shown in Figure 1(b) every air node has a corresponding solid mesh in the radial direction. Only part of the wall of thickness of 2mm is considered in the radial direction. At 2mm from the airway surface, the tissue is assumed to reach the body temperature as shown.

The solution sequence starts with an initial temperature of the body on all tissue nodes and that of ambient air on all the air nodes. At every time step, the convection-diffusion equation, Eq.7, is solved for all air nodes and the heat conduction equation, Eq.8, is solved for all solid nodes. At the interface between the solid and air nodes, the wall temperature is used from the tissue equation to solve air temperatures and air temperature is used to solve solid wall temperatures. The convergence of the wall temperature is important to obtain a valid solution. This is achieved by carrying out the calculations for a large number of breathing cycles.

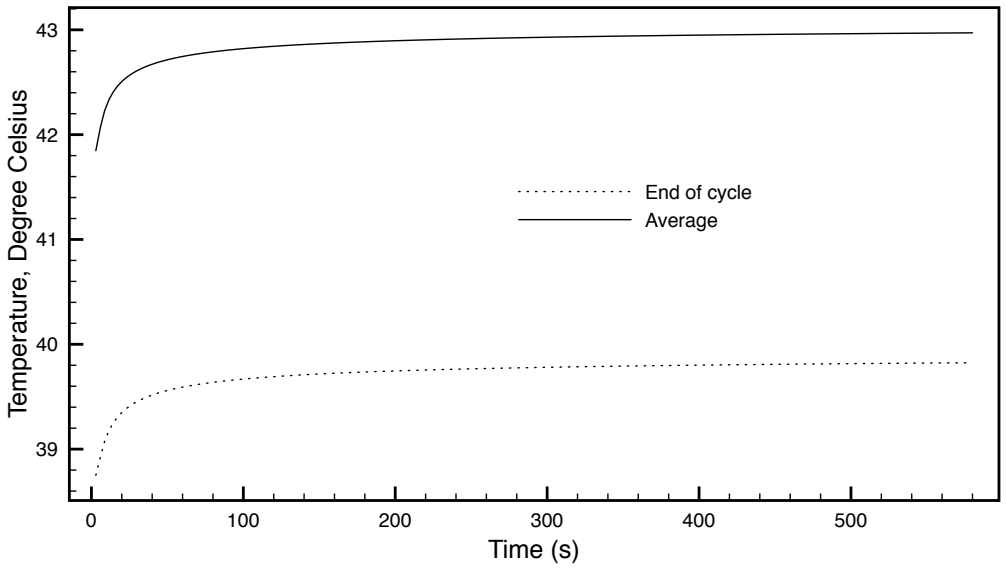

Figure 2: Convergence. Respiratory air temperature distribution at the end of each breathing cycle and average exit temperature plotted against time at an ambient temperature of 50^oC.

To make sure that the temperatures are converged to the right values, the calculations are carried out over a large number of breathing cycles, until the temperature change between two cycles is acceptably small as shown in Figure 2. As seen, about one hundred breathing cycles are needed to reach a converged state. Once such convergence is achieved, the uncertainties due to the initial conditions and the interface conditions are eliminated. In all the results presented in the present paper, at least two hundred breathing cycles were used.

4 RESULTS AND DISCUSSION

As shown in Figure 1, the respiratory system (Figure 1(a)) is approximated by a varying cross sectional area geometry as depicted in Figure 1(b). The varying cross sectional area is adopted from reference [43] and an approximate area variation with respiratory system length (staring from nose) is shown in Figure 1(c). The flow variation with time, during breathing, of an average human being is approximated from the measurements [44] and shown in Figure 1(d). Here, we assumed a breath rate of approximately 20 per minute representing an adult (2.9s per breath). Based the data gathered from the literature, the inlet flow variations and boundary conditions are imposed and solutions are obtained continuously for a number of breathing cycles. The converged final cycle results are used to plot the results presented below.

To make sure that the the initial transients are not influencing the final results, a convergence study in time was carried out as shown in Figure 2. The air temperatures are plotted at the end of each cycle in Figure 2. The average exit temperature over the last one third of the cycle is also plotted (referred to as 'average' in the figure). As seen, the results needed approximately one hundred breathing cycles to converge. In the remaining study we have used at least two hundred cycles to eliminate any errors associated with initial conditions. The mesh used contains very fine elements close to the inlet. Without a fine mesh close to the inlet, the calculations face an unstable solution. The parameters used in the calculations are:

- Body temperature - 36.8^oC
- Thermal capacity of air, $\rho_a c_{pa}$, - 1225 J/m^3K
- Thermal capacity of tissue, $\rho_t c_{pt}$, - 3.8×10^6 J/m^3K
- Heat transfer coefficient between the airway wall and air, h, - 0.2 W/m^{2o}K
- Thermal conductivity of air, k_a - 0.024 W/mK
- Thermal conductivity of tissue, k_t - 0.5 W/mK
- Latent heat of water evaporation, λ, - 2417.7 J/g
- Mol mass of water, M_w, - 18.016 g/mol
- Gas constant, R, - 8.3143 J/mol K

Figure 3 shows the relative importance of convection and evaporation heat transfer. In this figure the air temperature is plotted against the distance along the airway, starting from the inlet (nose). As seen the temperature distribution is dominated by evaporation heat transfer. The convection effect is very small compared to evaporation heat transfer. This very clearly confirms the experimental observation on animals[2].

Figures 4 (a) and (b) show the wall and air temperature variations over a breathing cycle at atmospheric temperatures of 20^oC and -20^oC respectively. The temperature values are plotted along the respiratory tract length at different times within a breathing cycle. At normal breathing conditions, the total duration of a breathing cycle assumed is 2.9s (see Figure 1(c)). The transient plots in Figure 4 shows the air and wall temperature distributions along the respiratory tract at 0.1s, 1.5s and 2.9s(0s). Up to 1.5s, the breathing cycle is in the inhalation phase and beyond 1.5s the exhalation starts. The temperature distributions shown in Figure 4 resemble a volume-pressure loop of the respiratory cycle.

Noting from Figure 4 that the temperature distributions at 2.9s is also the starting point of the breathing cycle, one can easily see the air temperature at 0.1s drops down to the ambient temperature in the vicinity of the inlet. At 1.5s (end point of inhalation), the air temperature drops down to its minimum value. At the exhalation phase, the temperature increases and reaches a maximum possible value for the given conditions. The wall temperature follows a similar pattern to that of the air temperature but with some distinctive differences. At 0.1s, the wall temperature has reduced along the length of the airway to reflect the sudden drop in inlet air temperature. This reduction in temperature is a result of inhalation air being at a lower temperature than the body temperature. This lower incoming temperature of the air starts reducing the wall

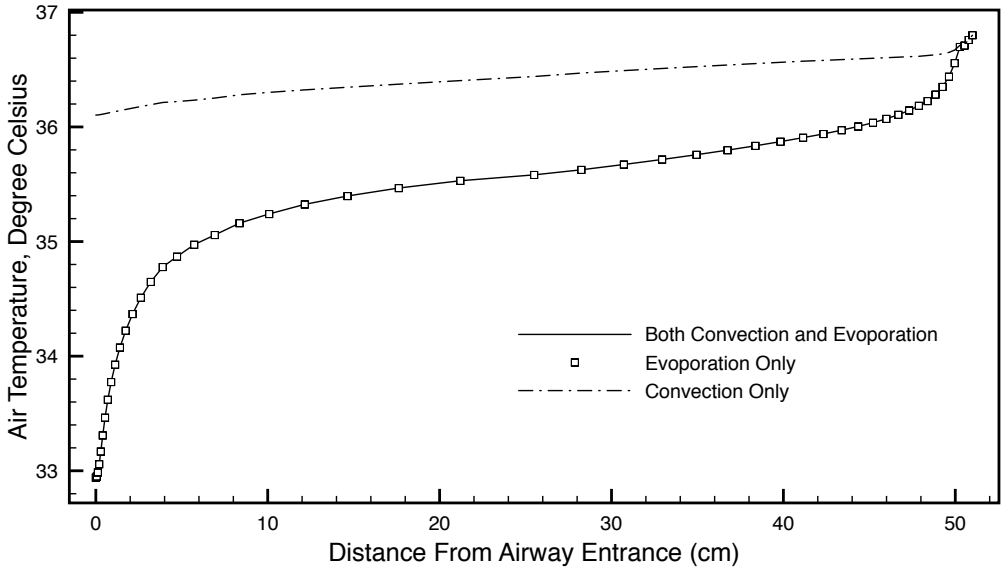

Figure 3: Respiratory air temperature distribution at the end of a breathing cycle. Comparison of temperature distributions with convection alone, evaporation alone and combined effect at an inlet temperature of 20^oC

temperature from the previous cycle and the wall temperature goes down further with the air temperature at 1.5s (end of inhalation). The wall temperature then substantially increases during exhalation and reaches its maximum value at 2.9s (end of exhalation and starting of inhalation). As seen the wall temperature at the end of exhalation is higher than that of the wall temperature at 0.1s but lower than the air temperature at the end of exhalation. This is due to the extreme dynamic nature and limited residence time of air along the wall. If more air residence time (extended exhalation) is available, the wall temperature is expected to approach the air temperature. It is also obvious from both Figures 4(a) and (b) that energy transport by air movement along the respiratory tract is more efficient and faster than the heat conduction in tissue. This is another reason why wall temperature is lower than air temperature at the end of exhalation. The exhalation of air is able to rapidly transport the body temperature from the lungs to the exist (inlet).

Figure 5 shows the comparison of air temperature values between the present and experimental data [2]. The experimental data shown are the exhalation temperature measured on sheep at different ambient temperatures. The assumption made in the present study is that the proposed model is applicable for any similar size respiratory systems. The temperature measured in the experiments probably are some form of averaged temperature values. The computed values however are obtained at the end of exhalation phase. As seen in the figure, the agreement between the computed and experimental data is very good at lower ambient temperatures for a human body (36.8^oC). The differences at higher ambient temperatures may be a result of a large number of unknown parameters. It is also important to note that the experimental valves are scattered over a range of temperature values and the best fitted data is used here to compare against numerical predctions.

Figure 5 also shows the results for a higher body temperature, measured on the animal model ([2] 39.8^oC). Although a better match with experimental data is obtained at larger ambient temperatures, the present results deviate from experimental data at lower ambient temperatures. The largest possible uncertainty in the calculations may arise due to the imprecise input of cross sectional and surface areas and some properties. Another major unknown parameter is the heat transfer coefficient between the wall and the air. This latter uncertainty may be small as the effect of convective heat transfer on temperature is very small compares to evaporation. The assumption that the temperature of tissue reaches the body temperature at a distance of 2mm from the wall may also contribute to the uncertainties in the temperature calculations.

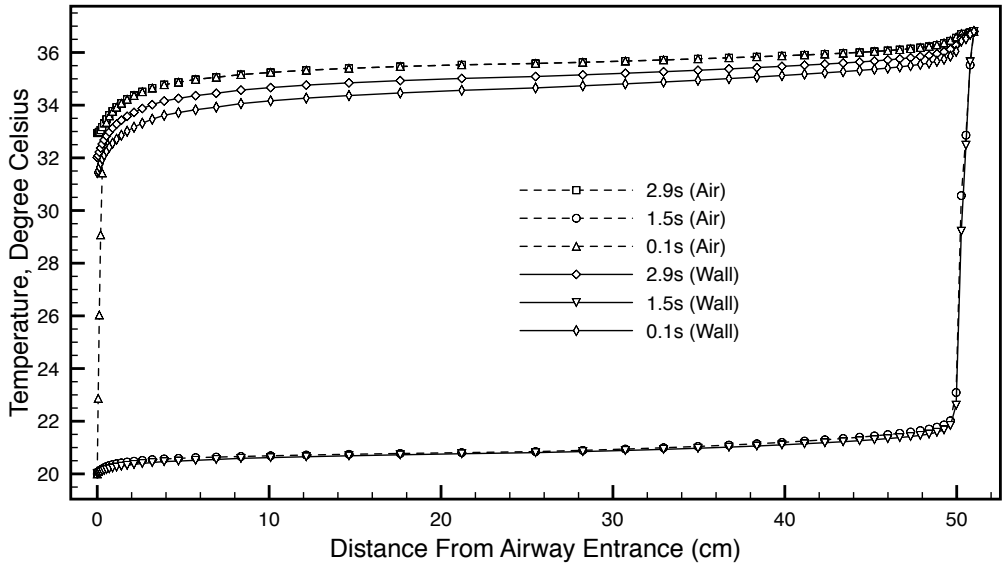

(a) Ambient temperature = 20^oC

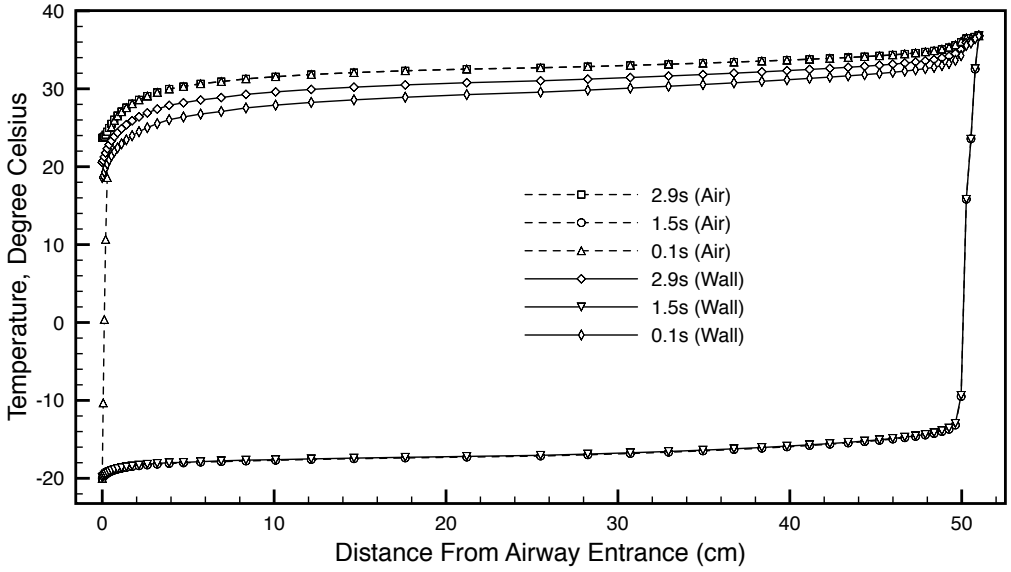

(b) Ambient temperature = -20^oC

Figure 4: Transient temperature variation of air and wall along the respiratory tract.

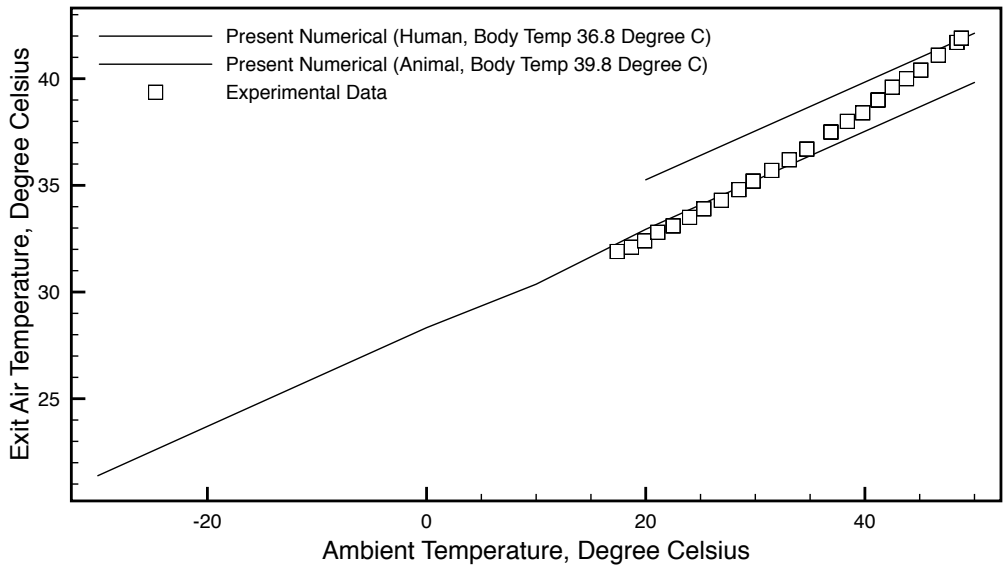

Figure 5: Exit temperature variation with respect to atmospheric temperature variation

Acknowledgement: This work is partially funded by EPSRC delivery plan and GCRF fundings

5 CONCLUSIONS

In the present work, an attempt has been made for the first time to computationally model the energy transport in a respiratory tract. Although the model presented is one-dimensional in nature, the results appear to be physically meaningful and they qualitatively reflect the data produced by animal experiments[2]. The results may be further refined by including thermoregulatory mechanisms in the soft tissue. The calculations may also be improved by incorporating models for structural motion and fluid dynamics. Since the present work was aimed at only demonstrating the new model, preference was not given to study effects of various pathologies. The present model provides the basis to study effect of respiratory tract related issues such as asthma (by modifying the heat transfer coefficient between the airway wall and air) and COPD (reduction in lung surface area).

References

[1] I. Madan, P. Bright, and M.R. Miller. Expired air temperature at the mouth during a maximal forced expiratory manoeuvre. *Eur Respir J*, 6:1556–1562, 1993.

[2] Roberto Gomes da Silva, Newton LaScala Jr, Alvaro Edison Lima Filho, and Marcelo Carlos Catharin. Respiratory heat loss in the sheep: a comprehensive model. *Int J Biometeorol*, 46:136–140, 2002.

[3] Brieva JL, Danta I, and Wanner A. Effect of an inhaled glucocorticosteroid on airway mucosal blood flow in mild asthma. *Am J Respir Crit Care Med*, 161:293–296, 2000.

[4] Payne DN, Adcock IM, Wilson NM, Oates T, Scallan M, and Bush A. Relationship between exhaled nitric oxide and mucosal eosinophilic inflammation in children with difficult asthma, after treatment with oral prednisolone. *Am J Respir Crit Care Med*, 164:1376–1381, 2001.

[5] P. Paredi, S.A. Kharitonov, and P.J. Barnes. Faster rise of exhaled breath temperature in asthma. a novel marker of airway inflammation? *American Journal of Respiratory and Critical Care Medicine*, 165:181–184, 2002.

[6] Zanconato S, Scollo M, Zaramella C, Landi L, Zacchello F, and Baraldi E. Exhaled carbon monoxide levels after a course of oral prednisone in children with asthma exacerbation. *J Allergy Clin Immunol*, 109:440–445, 2002.

[7] Piacentini GL, Bodini A, and Zerman L. Relationship between exhaled air temperature and exhaled nitric oxide in childhood asthma. *Eur Respir J*, 20:108–111, 2002.

[8] Paredi Paolo, Kharitonov Sergei A., and Barnes Peter J. Correlation of exhaled breath temperature with bronchial blood flow in asthma. *Respiratory Research*, 6:1–10, 2005.

[9] R. Jonston. Exhaled air temperature and asthma. http://www.pftforum.com/blog/exhaled-air-temperature-and-asthma/, January 2014.

[10] Popov TA, Dunev S, Kralimarkova TZ, Kraeva S, and Dubuske LM. Evaluation of a simple, potentially individual device for exhaled breath temperature measurement. *Respiratory Medicine*, 101:2044–2050, 2007.

[11] Sven Ingelstedt and Nils Gunnar Toremalm. Air flow patterns and heat transfer within the respiratory tract: A new method for experimental studies on models. *Acta Physiologica Scandinavica*, 51:204–217, 1961.

[12] G.W. Cole and N.R. Scott. A mathematical model of the dynamic heat transfer from the respiratory tract of a chicken. *Bulletin of Mathematical Biology*, 39:415 – 433, 1977.

[13] Iwajlo M. Kandjov. Heat and water rate transfer processes in the human respiratory tract at various altitudes. *Journal of Theoretical Biology*, 208:287 – 293, 2001.

[14] P Muthuganeisan. One-dimensional modelling of lung geometry. Erasmus Mundas MSc Thesis, Swansea University, 2009.

[15] Lorenz Berger, Rafel Bordas, Kelly Burrowes, Vicente Grau, Simon Tavener, and David Kay. A poroelastic model coupled to a fluid network with applications in lung modelling. *International Journal for Numerical Methods in Biomedical Engineering*, 32(DOI: 10.1002/cnm.2731), 2016.

[16] J.P. Mynard and P. Nithiarasu. A 1D arterial blood flow model incorporating ventricular pressure, aortic valve and regional coronary flow using locally conservative Galerkin (LCG) method. *Communications in Numerical Methods in Engineering*, 24:367–417, 2008.

[17] K. Low, R. van Loon, I. Sazonov, R. L. T. Bevan, and P. Nithiarasu. An improved baseline model for a human arterial network to study the impact of aneurysms on pressure-flow waveforms. *International Journal for Numerical Methods in Biomedical Engineering*, 28:1224–1246, 2012.

[18] Lucas O. Muller and Eleuterio F. Toro. Well-balanced high-order solver for blood flow in networks of vessels with variable properties. *International Journal for Numerical Methods in Biomedical Engineering*, 29:1388–1411, 2013.

[19] L.O. Müller and E.F. Toro. A global multiscale mathematical model for the human circulation with emphasis on the venous system. *International Journal for Numerical Methods in Biomedical Engineering*, 30:681–725, 2014.

[20] Jordi Alastruey, Anthony A. E. Hunt, and Peter D. Weinberg. Novel wave intensity analysis of arterial pulse wave propagation accounting for peripheral reflections. *International Journal for Numerical Methods in Biomedical Engineering*, 30(DOI: 10.1002/cnm.2602):249–279, 2014.

[21] J. M. T. Keijsers, C. A. D. Leguy, W. Huberts, A. J. Narracott, J. Rittweger, and F. N van de Vosse. A 1d pulse wave propagation model of the hemodynamics of calf muscle pump function. *International Journal for Numerical Methods in Biomedical Engineering*, 31(DOI: 10.1002/cnm.2714), 2015.

[22] Jonathan P. Mynard and Kristian Valen-Sendstad. A unified method for estimating pressure losses at vascular junctions. *International Journal for Numerical Methods in Biomedical Engineering*, 31(DOI: 10.1002/cnm.2717), 2015.

[23] P. G. Huang and L. O. Muller. Simulation of one-dimensional blood flow in networks of human vessels using a novel tvd scheme. *International Journal for Numerical Methods in Biomedical Engineering*, 31:DOI: 10.1002/cnm.2701, 2015.

[24] Paulo Roberto Trenhago, Luciano Goncalves Fernandes, Lucas Omar Muller, Pablo Javier Blanco, and Raul Antonino Feijo. An integrated mathematical model of the cardiovascular and respiratory systems. *International Journal for Numerical Methods in Biomedical Engineering*, 32(DOI: 10.1002/cnm.2736), 2015.

[25] E. Boileau, P. Nithiarasu, J.B. Blanco, L.O. Muller, F. E.E. Fossans, L.R. Helleviks, W.P. Doners, W. Huberts, M. Willemet, and J. Alastruey. A benchmark study of 1-d numerical schemes for arterial blood flow modelling. *International Journal for Numerical Methods in Biomedical Engineering*, e02732(DOI: 10.1002/cnm.2732), 2015.

[26] Jason Carson and Raoul Van Loon. An implicit solver for 1d arterial network models. *International Journal for Numerical Methods in Biomedical Engineering*, 10.1002/cnm.2837, 2016.

[27] Lucas O. Muller, Pablo J. Blanco, Sansuke M. Watanabe, and Raul A Feijo. A high-order local time stepping finite volume solver for one-dimensional blood flow simulations: application to the adan model. *International Journal for Numerical Methods in Biomedical Engineering*, 32(DOI: 10.1002/cnm.2761), 2016.

[28] A. Danilov, Yu. Ivanov, R. Pryamonosov, and Yu. Vassilevski. Methods of graph network reconstruction in personalized medicine. *International Journal for Numerical Methods in Biomedical Engineering*, 32(DOI: 10.1002/cnm.2754), 2016.

[29] A. Coccarelli and P. Nithiarasu. A robust finite element modelling approach to conjugate heat transfer in flexible elastic tubes and tube networks. *Numerical Heat Transfer, Part A Applications*, 67:513–530, 2015.

[30] A. Coccarelli, E. Boileau, D. Parthimos, and P. Nithiarasu. An advanced computational bioheat transfer model for a human body with an embedded systemic circulation. *Biomechanics and Modeling in Mechanobiology*, 15(5)(DOI: 10.1007/s10237-015-0751-4):1173–1190, 2016.

[31] P. Nithiarasu, C. B. Liu, and N. Massarotti. Laminar and turbulent flow calculations through a model human upper airway using unstructured meshes. *Communications in Numerical Methods in Engineering*, 23(12):1057+, 2007.

[32] P. Nithiarasu, O. Hassan, K. Morgan, N. P. Weatherill, C. Fielder, H. Whittet, P. Ebden, and K. R. Lewis. Steady flow through a realistic human upper airway geometry. *International Journal for Numerical Methods in Fluids*, 57:631–651, 2008.

[33] Kambiz Farahmand, Raghavan Srinivasan, and Mohsen Hamidi. Cfd heat transfer simulation of the human upper respiratory tract for oronasal breathing condition. *International Journal of Indus trial Engineering Computations*, 3:63–70, 2012.

[34] P. H. Saksono, P. Nithiarasu, I. Sazonov, and S. Y. Yeo. Computational flow studies in a subject-specific human upper airway using a one-equation turbulence model. Influence of the nasal cavity. *International Journal for Numerical Methods in Engineering*, 87:96–114, 2011.

[35] Prihambodo H. Saksono, Perumal Nithiarasu, and Igor Sazonov. Numerical Prediction of Heat Transfer Patterns in a Subject-Specific Human Upper Airway. *Journal of Heat Transfer - Transactions of ASME*, 134, 2012.

[36] Christian J. Roth, Mahmoud Ismail, Lena Yoshihara, and Wolfgang A. Wall. A comprehensive computational human lung model incorporating inter-acinar dependencies: Application to spontaneous breathing and mechanical ventilation. *International Journal for Numerical Methods in Biomedical Engineering*, (DOI: 10.1002/cnm.2787), 2016.

[37] Francesc Verdugo, Christian J. Roth, Lena Yoshihara, and Wolfgang A. Wall. Efficient solvers for coupled models in respiratory mechanics. *International Journal for Numerical Methods in Biomedical Engineering*, (DOI: 10.1002/cnm.2795), 2016.

[38] P. Nithiarasu, R.W. Lewis, and K.N. Seetharamu. *Fundamentas of the finite element method for heat, mass and fluid flow.* Wiley, second edition, 2016.

[39] Chapman AJ. *Fundamentals of heat transfer.* MacMillan, New York, 1987.

[40] Monteith JL and Unsworth MH. *Principles of environmental physics.* Edward Arnold, London, 1991.

[41] McArthur A J. Thermal interaction between animal and microclimate: a comprehensive model. *J Theor Biol*, 126:203– 238, 1987.

[42] O. C. Zienkiewicz, R. L. Taylor, and P. Nithiarasu. *The Finite Element Method for Fluid Dynamics.* Elsevier, seventh edition, 2014.

[43] E.R. Weibel. Morphometry of the human lung. *Science*, pages 115–126, 1963.

[44] J.K. Gupta, C.-H. Lin, and Q.X. Chen. Characterizing exhaled airflow from breathing and talking. *Indoor Air*, 20:31–39., 2010.